

Title	Microstructure of Polycrystalline Silicon Films Formed through Explosive Crystallization Induced by Flash Lamp Annealing
Author(s)	Ohdaira, Keisuke; Ishii, Shohei; Tomura, Naohito; Matsumura, Hideki
Citation	Japanese Journal of Applied Physics, 50: 04DP01-1-04DP01-3
Issue Date	2011
Type	Journal Article
Text version	author
URL	<a href="http://hdl.handle.net/10119/9864">http://hdl.handle.net/10119/9864</a>
Rights	This is the author's version of the work. It is posted here by permission of The Japan Society of Applied Physics. Copyright (C) 2011 The Japan Society of Applied Physics. Keisuke Ohdaira, Shohei Ishii, Naohito Tomura, and Hideki Matsumura, Japanese Journal of Applied Physics, 50, 2011, 04DP01-1-04DP01-3. <a href="http://jjap.jsap.jp/link?JJAP/50/04DP01/">http://jjap.jsap.jp/link?JJAP/50/04DP01/</a>
Description	

# **Microstructure of Polycrystalline Silicon Films Formed through Explosive Crystallization Induced by Flash Lamp Annealing**

Keisuke Ohdaira<sup>1,2</sup>, Shohei Ishii<sup>1</sup>, Naohito Tomura<sup>1</sup>, and Hideki Matsumura<sup>1</sup>

<sup>1</sup>Japan Advanced Institute of Science and Technology (JAIST),

1-1 Asahidai, Nomi, Ishikawa 923-1292, Japan

<sup>2</sup>PRESTO, Japan Science and Technology Agency (JST),

4-1-8 Honcho, Kawaguchi, Saitama 332-0012, Japan

E-mail: ohdaira@jaist.ac.jp

## Abstract

We perform transmission electron microscopy investigation of the microstructures of polycrystalline silicon (poly-Si) films formed through explosive crystallization (EC) induced by flash lamp annealing (FLA) of precursor amorphous silicon (a-Si) films. Two characteristic regions, formed periodically as a result of EC, show different microstructures: one consists of randomly oriented, densely packed fine grains of approximately 10 nm in size, whereas the other has relatively large (>100 nm), stretched grains, probably formed through liquid-phase epitaxy onto solid-phase-nucleated grains. Little a-Si tissue surrounding grains can be observed in the lattice images of flash-lamp-crystallized poly-Si films, which would be favorable for the rapid transport of photocarriers.

## 1. Introduction

Thin crystalline silicon (c-Si) films are promising as a next-generation solar cell material. Solar cells with a high conversion efficiency (>10%) have been demonstrated using polycrystalline (poly-Si) films formed by solid-phase crystallization (SPC) of precursor amorphous silicon (a-Si) films on glass substrates by furnace annealing for several hours.<sup>1)</sup> Such a time-consuming crystallization is, however, unfavorable for mass production in which high throughput is required, and therefore, a rapid crystallization technique is desired. Furthermore, careful tuning of the annealing duration will lead to selective heating of the precursor a-Si films only, keeping the temperature of low-cost glass substrates with poor thermal tolerance sufficiently low.

Flash lamp annealing (FLA) is an annealing technique using a light pulse of a few milliseconds and can crystallize micrometer-thick a-Si films without heating of the whole glass substrate owing to its appropriate annealing duration.<sup>2,3)</sup> We have demonstrated that FLA can yield 4.5- $\mu\text{m}$ -thick poly-Si films even on soda lime glass substrates.<sup>4)</sup> The flash-lamp-crystallized (FLC) poly-Si films can be processed to solar cells that demonstrate rectifying and photovoltaic properties.<sup>5)</sup> We have also clarified that the flash-lamp-induced crystallization progresses laterally through explosive crystallization (EC), that is, autocatalytic crystallization associated with the liberation of latent heat.<sup>6)</sup> The EC induced by FLA leaves behind periodic structures along the lateral crystallization directions under certain film and FLA conditions.<sup>7,8)</sup> The FLC poly-Si films have two characteristic regions with different features, such as grain size and surface morphology, resulting in the formation of the periodic structures.<sup>7)</sup> In this study, we have investigated the microstructures of FLC poly-Si films in detail by means of cross-sectional transmission electron microscopy (TEM) and electron beam diffraction

(EBD) patterns to gain further understanding of the microstructures of FLC poly-Si films and their crystallization mechanisms.

## **2. Experimental Procedure**

First, Cr films of 60 nm thickness were sputtered, with the aim of suppressing Si film peeling during FLA, on quartz glass substrates of  $20 \times 20 \times 0.7$  mm<sup>3</sup>, followed by the deposition of 4.5- $\mu$ m-thick a-Si films by catalytic chemical vapor deposition (Cat-CVD). The detailed deposition conditions have been summarized elsewhere.<sup>9)</sup>

FLA was performed with a pulse duration of 5 ms and irradiance of approximately 20 J/cm<sup>2</sup>. Flash-lamp light illuminated the whole area of the substrates with sufficient areal homogeneity of within 5%. Only one shot of flash irradiation was performed for one sample. No additional heating was applied to samples during FLA. TEM observation was performed using a high-resolution electron microscope (JEOL JEM-4000EX) with an electron energy of 400 keV after focused-ion-beam thinning.

## **3. Results and Discussion**

In this study, we selected a partially crystallized Si film sample for cross-sectional TEM observation. The surface appearance of the FLC poly-Si film is shown in Fig. 1, and indicates that lateral crystallization is ignited at film edges and the crystallized area expands towards the center. A cross section for TEM observation was formed at an a-Si/c-Si boundary. According to the results of Raman spectroscopy, the crystallized parts have high crystalline fractions close to unity, which is consistent with those reported previously.<sup>4,7)</sup>

Figure 2 shows the low-magnification cross-sectional TEM image of the FLC

poly-Si film. One can clearly see two characteristic regions in the image: a region containing surface protrusions and relatively large, stretched grains with sizes of more than 100 nm (large-grain region), and a region with a flat surface and containing no 100-nm-sized large grains (fine-grain region). EBD patterns of the two regions, also shown in Fig. 2, reveal that the former has a higher degree of orientation than the latter. The EBD pattern at position c, within 1  $\mu\text{m}$  from the a-Si/c-Si boundary, indicates a complete halo ring, indicating quite abrupt phase change from c-Si to a-Si at the boundary.

Figures 3(a) and 3(b) show the bright- and dark-field images of the fine-grain region of the FLC poly-Si film. These images clearly show the existence of 10-nm-sized fine grains, which is consistent with the grain size estimated from the full width at half-maximum (FWHM) of a c-Si Raman peak.<sup>4,10</sup> Figure 3(c) shows the lattice image of the fine-grain region. One can confirm individual grains in the image, whereas the amorphous phase is negligible between them. The random orientation of grains in FLC poly-Si films has also been confirmed in an X-ray diffraction (XRD) pattern<sup>11</sup>. According to these results, it is found that the fine-grain regions consist of randomly oriented, densely packed fine grains with little amorphous phase.

Figures 4(a) and 4(b) show bright- and dark-field images of the large-grain region of the FLC poly-Si film. In contrast to the fine-grain region, large grains of over 100 nm are clearly seen. The dark-field image reveals no significant variation of orientation inside the large grain, which probably indicates that the large grains are formed through epitaxial growth onto one nucleus. Figure 4(c) shows the lattice image of the large-grain region of the FLC poly-Si film. No clear grain boundaries are seen in the image. This is also an indication of the formation of large grains.

The relatively large grains stretching along the crystallization direction are probably formed through liquid-phase epitaxy (LPE) of molten Si onto solid-phase-nucleated grains. The formation of surface protrusions cannot be explained by complete SPC, and thus, the large-grain regions are at least partially melted during crystallization. Since the melting point of a-Si is about 1418 K,<sup>2)</sup> the partially melted Si undergoes a maximum supercooling of 269 K in this system, at which the homogeneous Si nucleation rate is estimated to be less than  $1 \text{ m}^{-3} \text{ s}^{-1}$ .<sup>12)</sup> This indicates that nucleation occurs in the solid phase even in the large-grain regions undergoing partial melting. The molten Si then contributes to the enlargement of the solid-phase-nucleated grains through LPE, and the speed of epitaxial growth can be spatially inhomogeneous because of a thermal gradient in the lateral direction in the vicinity of the a-Si/c-Si interface during EC. At temperatures around the melting point of a-Si of 1418 K, the epitaxial growth speed increases with decreasing temperature.<sup>2)</sup> This results in the faster epitaxial growth near the a-Si/c-Si interface where the temperature is lower and the formation of grains stretching along the lateral crystallization direction.

From the point of view of solar cell application, the FLC poly-Si with a high crystalline fraction would lead to the rapid transport of photogenerated carriers. Relatively high Hall mobilities of  $\sim 10 \text{ cm}^2 \text{ V}^{-1} \text{ s}^{-1}$  have actually been observed in the FLC poly-Si films.<sup>13)</sup> Effective carrier collection can be expected in solar cells fabricated using FLC poly-Si films. On the other hand, the passivation of grain boundaries would be one of the most important issues in realizing high-efficiency solar cells using FLC poly-Si films, because of the absence of a-Si tissue passivating grain boundaries, unlike CVD microcrystalline Si films. The issue would be overcome by terminating dangling bonds at grain boundaries with H atoms that are present at about  $10^{21} \text{ atoms/cm}^3$  in FLC

poly-Si films. This high H density is due to the suppression of H desorption during FLA, which may result from the rapid lateral thermal transfer in EC. We have found that these remaining H atoms can be utilized for the termination of Si dangling bonds by furnace annealing,<sup>14)</sup> and the defect density can be decreased to  $\sim 5 \times 10^{16} \text{ cm}^{-3}$ .<sup>15)</sup> This value is close to those of CVD a-Si and microcrystalline Si films, and further reduction of defect density will hopefully be realized by optimizing the defect-terminating annealing conditions and/or applying other passivation techniques.

#### **4. Conclusions**

High-resolution TEM observations have clarified the difference in the microstructures of fine-grain and large-grain regions of FLC poly-Si films. The fine-grain region consists of randomly oriented, densely packed fine grains of approximately 10 nm in size, whereas large-grain regions have stretched grains, probably formed through liquid-phase epitaxy onto solid-phase-nucleated grains. The characteristic microstructures without a-Si tissue around the grains would lead to better carrier transport properties than those of a-Si and  $\mu\text{c-Si}$ , whereas the passivation of grain boundaries would be one of the key issues in the realization of high-performance solar cells.

#### **Acknowledgements**

The authors acknowledge T. Owada and T. Yokomori of Ushio Inc. for their expert work in FLA, and T. Yoshida of JAIST for his support in experiments. This work was supported by the JST PRESTO program.

## References

- 1) M. J. Keevers, T. L. Young, U. Schubert, and M. A. Green: Proc. 22nd European Photovoltaic Solar Energy Conf., 2007, p. 1783, and references therein.
- 2) M. Smith, R. McMahon, M. Voelskow, D. Panknin, and W. Skorupa: J. Cryst. Growth **285** (2005) 249.
- 3) H. Habuka, A. Hara, T. Karasawa, and M. Yoshioka: Jpn. J. Appl. Phys. **46** (2007) 937.
- 4) K. Ohdaira, T. Fujiwara, Y. Endo, S. Nishizaki, and H. Matsumura: Jpn. J. Appl. Phys. **47** (2008) 8239.
- 5) K. Ohdaira, T. Fujiwara, Y. Endo, K. Shiba, H. Takemoto, and H. Matsumura: Jpn. J. Appl. Phys. **49** (2010) 04DP04.
- 6) H. -D. Geiler, E. Glaser, G. Götz, and M. Wagner: J. Appl. Phys. **59** (1986) 3091.
- 7) K. Ohdaira, T. Fujiwara, Y. Endo, S. Nishizaki, and H. Matsumura: J. Appl. Phys. **106** (2009) 044907.
- 8) K. Ohdaira, T. Nishikawa, and H. Matsumura: J. Cryst. Growth **312** (2010) 2834.
- 9) K. Ohdaira, S. Nishizaki, Y. Endo, T. Fujiwara, N. Usami, K. Nakajima, and H. Matsumura: Jpn. J. Appl. Phys. **46** (2007) 7198.
- 10) K. Ohdaira, Y. Endo, T. Fujiwara, S. Nishizaki, and H. Matsumura: Jpn. J. Appl. Phys. **46** (2007) 7603.
- 11) K. Ohdaira, H. Takemoto, T. Nishikawa, and H. Matsumura: Curr. Appl. Phys. **10** (2010) S402.
- 12) R. P. Liu, T. Volkmann, and D. M. Herlach: Acta Mater. **49** (2001) 439.
- 13) K. Ohdaira, T. Nishikawa, S. Ishii, N. Tomura, and H. Matsumura: to be published in Proc. 35th IEEE Photovoltaic Specialists Conf., 2010.



- 14) K. Ohdaira, H. Takemoto, K. Shiba, and H. Matsumura: Appl. Phys. Express **2** (2009) 061201.
- 15) K. Ohdaira, T. Nishikawa, S. Ishii, N. Tomura, K. Koyama, and H. Matsumura: Proc. 5th World Conf. Photovoltaic Energy Conversion, 2010, p. 3546.

## Figure captions

Fig. 1 Surface appearance of FLC poly-Si film used for TEM observation. The position of the cross section is also indicated.

Fig. 2 Cross-sectional TEM image (bright field) of the FLC poly-Si film. Straight and dashed arrows indicate the large-grain and fine-grain regions, respectively. EBD patterns recorded at (a) fine-grain, (b) large-grain, and (c) amorphous regions are also shown.

Fig. 3 TEM images of the fine-grain region of the FLC poly-Si film: (a) bright-field image, (b) dark-field image, and (c) lattice image.

Fig. 4 TEM images of the large-grain region of the FLC poly-Si film: (a) bright-field image, (b) dark-field image, and (c) lattice image.

## Cross section

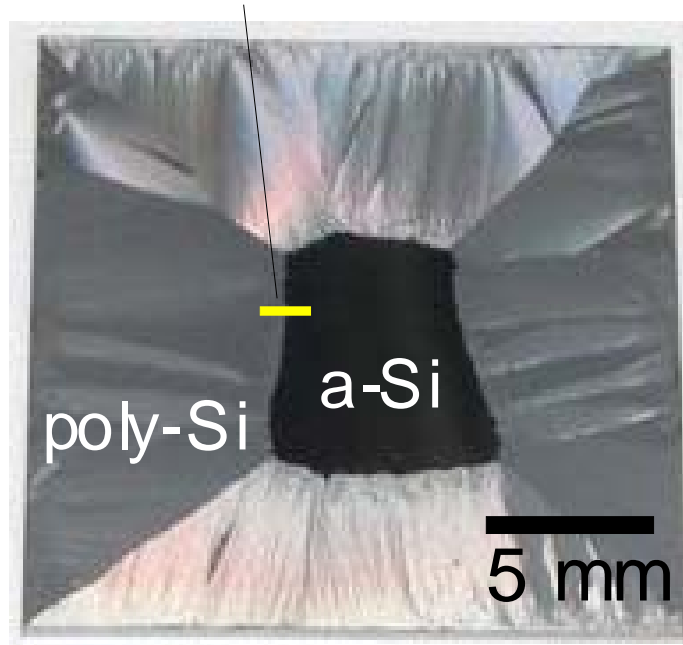


Fig. 1 K. Ohdaira *et al.*,

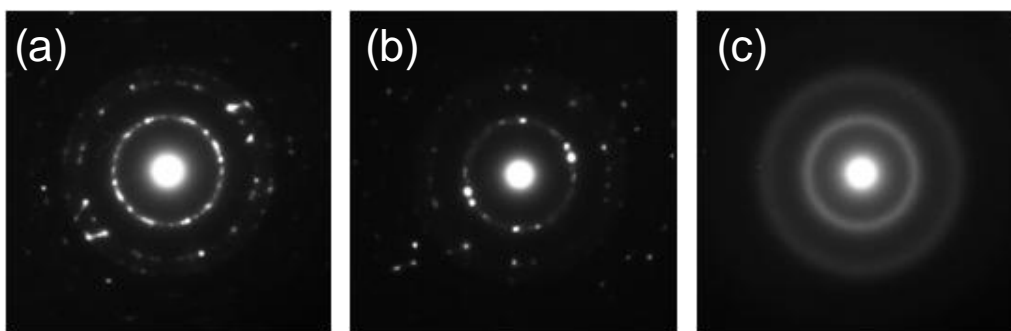
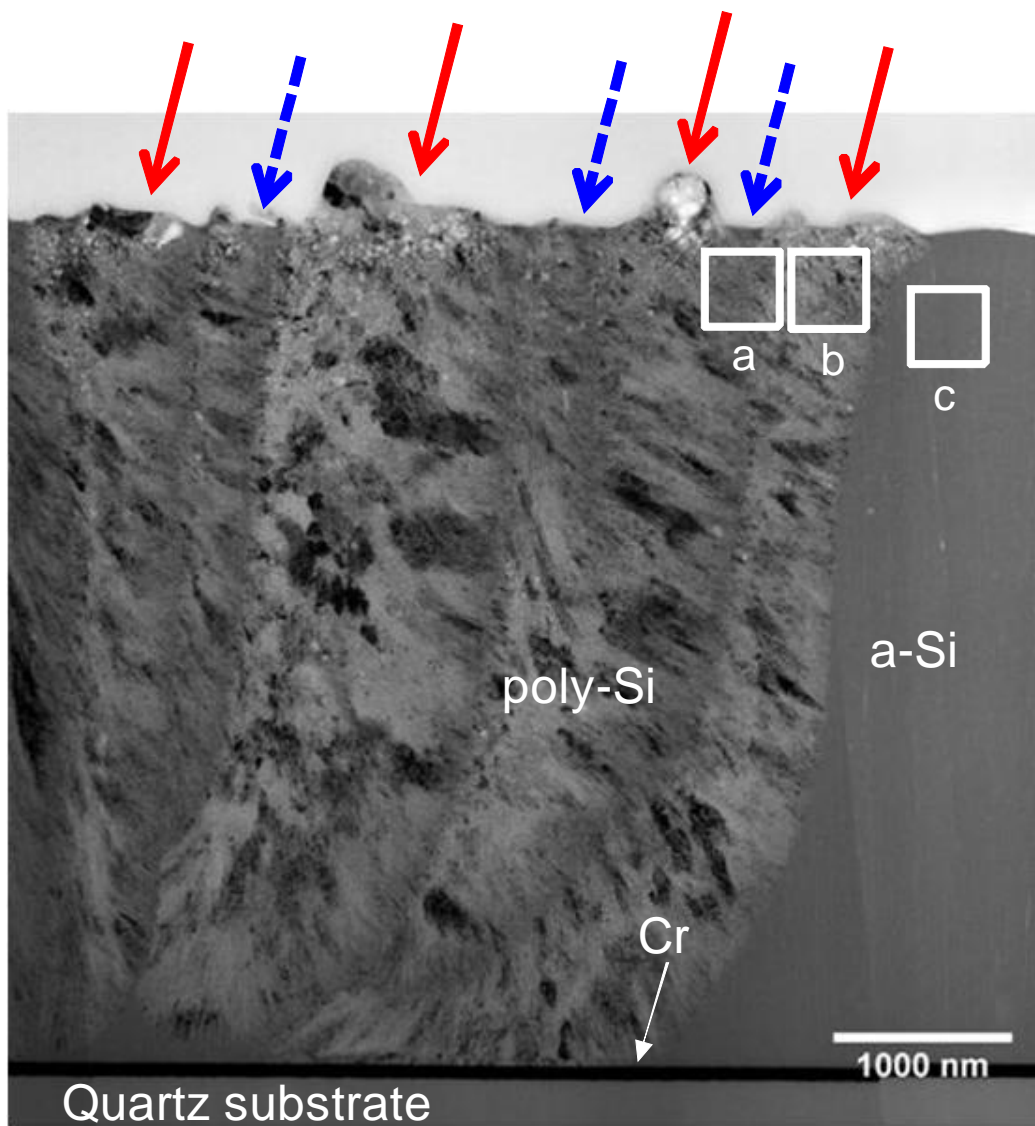


Fig. 2 K. Ohdaira *et al.*,

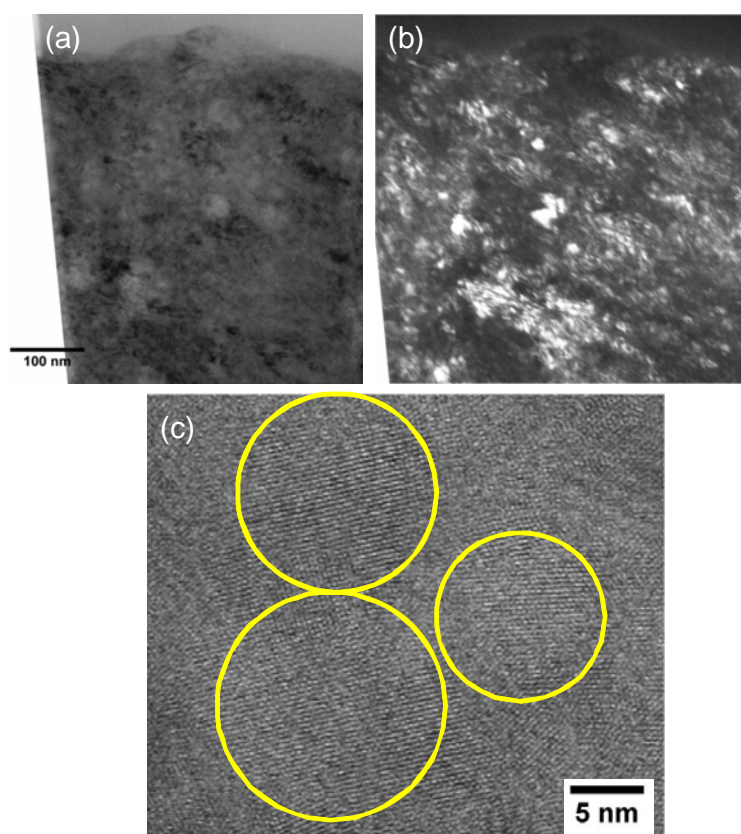


Fig. 3 K. Ohdaira *et al.*,

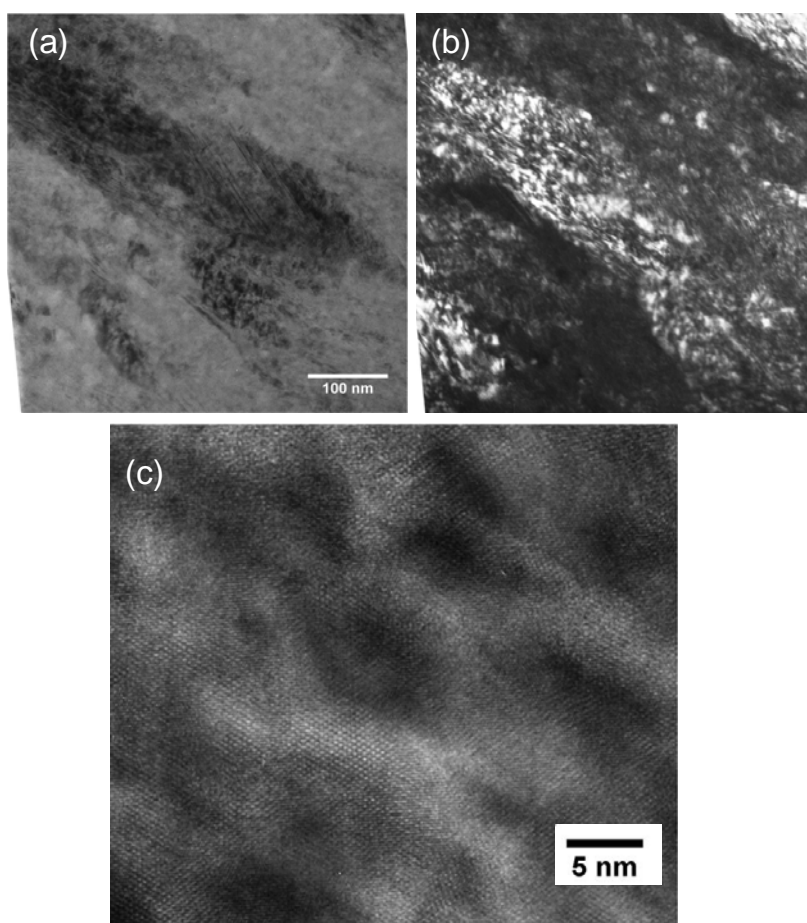


Fig. 4 K. Ohdaira *et al.*,